Deexcitation and recombination of excited ions through doubly excited levels in a dense recombining plasma: Lithiumlike recombining plasma laser

Tetsuya Kawachi
The Institute of Physical and Chemical Research (RIKEN), Saitama, 351-01, Japan

Takashi Fujimoto
Department of Engineering Science, Kyoto University, Kyoto, 606-01, Japan

(Received 8 July 1996)

Collisional transitions from excited levels in a dense recombining plasma have been considered for lithiumlike ions. Deexcitation from a level of the lithiumlike ion is enhanced by a process in which berylliumlike ions in doubly excited levels in local thermodynamic equilibrium with respect to this level autoionize. Excited ions may recombine through a process similar to the collisional-radiative (CR) recombination as in the case of ions in their ground states. We have estimated the effective rate coefficients for these processes by adopting various approximations. We have incorporated these approximations into our CR model code for lithiumlike aluminum ions in a high-density recombining plasma. The excited level populations and the amplification gains of several laser transitions are calculated for typical conditions of the recombining plasma laser. For an electron temperature of 5 eV, the gains of the $3d\ ^2D-5f\ ^2F$ and $3d\ ^2D-4f\ ^2F$ transitions are consistent with the experimental results. [S1063-651X(97)06901-8]

PACS number(s): 52.20.−j

I. INTRODUCTION

The recent development of high irradiance lasers makes it possible to produce dense and hot plasmas. The use of these plasmas in a soft-x-ray laser, a high irradiance x-ray source, or inertial-confinement fusion research requires as good an understanding as possible of the population kinetics of the ions in excited levels under the specific plasma conditions. At electron densities (n_e) of the order of 10^{24}–10^{27} m^{-3}, the number of ions populated in doubly excited levels is substantial, and the atomic processes involving these levels may play an important role in the population kinetics of the singly excited ions. One of the processes relevant in this context was proposed by Fujimoto and Kato [1,2]: hydrogenlike ions may be excited via doubly excited heliumlike ions that are created by dielectronic capture of the hydrogenlike ions. They also proposed the corresponding deexcitation process. They named these processes ''dielectronic capture and ladderlike (DL) excitation and deexcitation'' and showed that the processes enhanced the effective excitation and deexcitation rate coefficients in dense plasmas.

Moreover, in dense plasmas other processes such as the recombination of excited ions, which also involve doubly excited levels, may also be significant. It is therefore worth examining the effect of these additional processes on the population kinetics of singly excited ions in dense plasmas. Recently, lithiumlike aluminum ions produced in a recombining plasma have been studied in soft-x-ray laser experiments [3–5]. A serious discrepancy between the experiments and the collisional-radiative model calculations has been pointed out for the gain of the $3d\ ^2D-5f\ ^2F$ transition [6,7]: the calculated gain is smaller by one or two orders of magnitude than the experimental values. These calculations did not account for these additional processes. In the present work, we examine the effects of these additional processes on the populations of excited lithiumlike aluminum ions and on the gains of the laser transitions.

When we deal with doubly excited levels of an ion, we face the difficulty of a very large number of doubly excited levels existing with various configurations and symmetries, interacting with each other and with the underlying continuum states. Constructing wave functions of all these levels and diagonalizing them would obviously be impractical. Since our present objective is not to examine these individual levels and their populations, but rather their effects on the population kinetics of the singly excited ions, we shall adopt the following simple approximations: (i) we treat a doubly excited berylliumlike ion as consisting of an excited lithiumlike ion core and another excited electron (which we call the captured electron) in quasi-hydrogenic levels and (ii) we take into account the autoionization and dielectronic capture processes and ignore other possible interactions.

Our present treatment may be justified as follows: We are concerned with a dense plasma, and frequency inelastic collisions tend to redistribute the populations among the doubly excited levels according to their statistical weights [8]. Thus any effects arising from the characteristics of individual levels tend to be smoothed out.

II. DL EXCITATION AND DEEXCITATION

The DL excitation of $i \rightarrow k$ in lithiumlike ions may be described, in the present approximation, as a series of processes of the dielectronic capture of an electron by a lithiumlike ion in level i to form a berylliumlike ion in doubly excited level (k,p), followed by the ladderlike excitation-ionization [9], resulting in the lithiumlike ion in level k [2], viz.,

$$A^{q+}(i)+e \rightarrow A^{(q-1)+}(k,p) \rightarrow A^{(q-1)+}(k,p+1) \rightarrow A^{(q-1)+}(k,p+2) \rightarrow \cdots \rightarrow A^{q+}(k)+e, \quad (1)$$

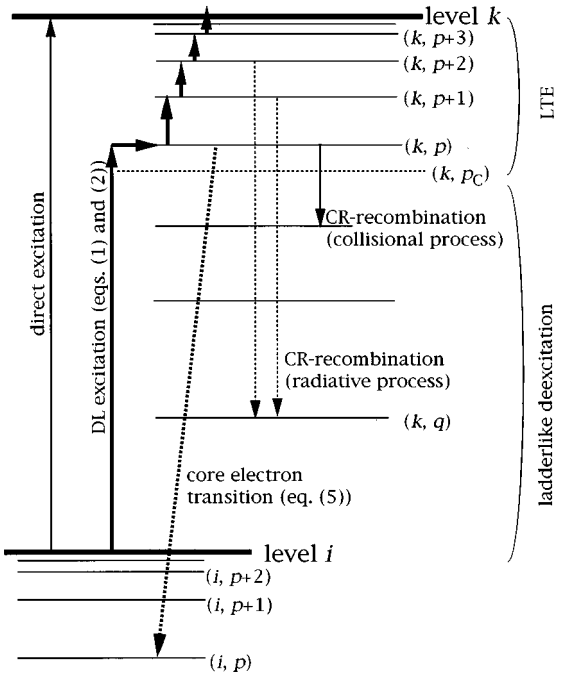

FIG. 1. Schematic diagram of the DL excitation (thick solid arrows), core electron transition (thick dotted arrow), and CR recombination of excited ions by radiation (thin dotted downward arrows) and by collision (thin solid downward arrow).

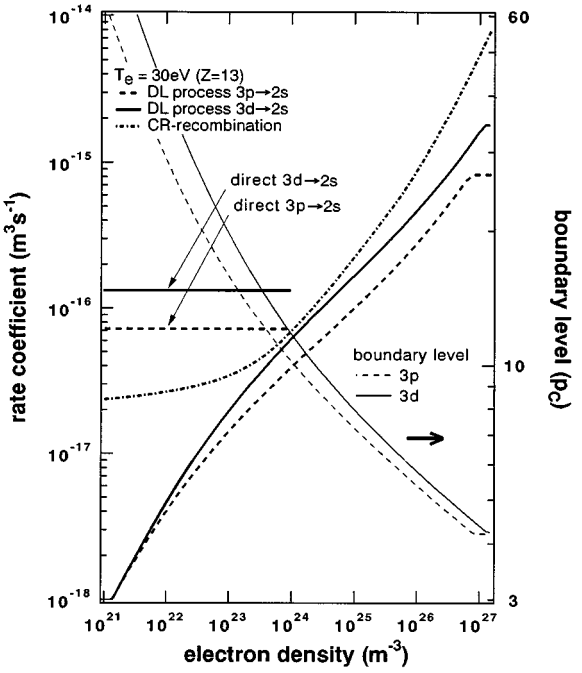

FIG. 2. Thin solid and dotted lines, the principal quantum number of the generalized Griem boundary or Byron boundary level for the $(3p\ ^2P,p)$ and the $(3d\ ^2D,d)$ doubly excited levels, respectively. DL deexcitation for the $3p\ ^2P \rightarrow 2s\ ^2S$ (thick solid line) and the $3d\ ^2D \rightarrow 2s\ ^2S$ (thick dotted line). Thick dash-dotted line, the recombination rate coefficient from an excited level. The rate coefficients for the DL deexcitation and recombination are labeled on the left-hand side ordinate and the boundary levels are on the right-hand side ordinate. The direct deexcitation rate coefficients are shown by the horizontal lines. $T_e = 30$ eV.

where e denotes an electron and p denotes the captured electron state with its principal quantum number p. A schematic diagram of this process is shown in Fig. 1 (thick solid arrows). This sequence of processes represents a ''virtual'' contribution to the excitation $i \rightarrow k$, to be added to the ordinary direct excitation. The effective excitation rate coefficient is approximately given as

$$C_{\mathrm{DL}}(i,k) = \int_{p_C}^{\infty} r_d(i;k,p)\,dp, \tag{2}$$

where $r_d(i;k,p)$ is the dielectronic capture rate coefficient from i to (k,p) and p_C is the lower end of the excitation ladder. p_C is given either by the generalization of Griem's boundary level p_G [10] or Byron's boundary level p_B [11], whichever is larger [2,12]: For the doubly excited levels lying above (k,p_G), the dominant depopulation process is the collisional excitation or deexcitation, while for levels lying below that, the dominant process is autoionization or radiative decay. For the levels lying above (k,p_B) the dominant collisional depopulation process is excitation, while for the levels below that it is deexcitation. In Fig. 2, the thin solid and dotted lines represent the boundary level for the $(3p\ ^2P,p)$ and $(3d\ ^2D,p)$ levels of aluminum, respectively. $T_e = 30$ eV has been assumed. For $n_e \leqslant 10^{27}\ \mathrm{m}^{-3}$, p_C is given by p_G, while for higher densities it is given by p_B $(=4.2)$ [12]. Since the dielectronic capture cross section across the excitation threshold to the excitation cross section is a continuous function of energy, Eq. (2) can be approximated as

$$C_{\mathrm{DL}}(i \rightarrow k) = \int_{E_C}^{E(i,k)} \sigma(i \rightarrow k;E) f(E) v\ dE, \tag{3}$$

where E_C is the energy of the boundary level (k,p_C), which is measured from the energy of level i, $\sigma(i \rightarrow k;E)$ is the excitation cross section extrapolated below the excitation threshold $E(i,k)$, v is the velocity of the incoming electron, and $f(E)$ is the energy distribution function of electrons. In the following the Maxwell distribution with electron temperature T_e will be assumed.

In a recombining plasma the population in level k is accompanied by populations in level (k,p); the high-lying doubly excited levels with large p are coupled so strongly with the continuum states $(k+e)$ that the populations of these levels are given by their local thermodynamic equilibrium (LTE) values. The lower limit of the levels having LTE populations is also given by p_C [12]. These populations may be lost by autoionization $(k,p) \rightarrow i + e (i < k)$, where i lies energetically lower than level k. The populations lost by this process are rapidly supplied by recombination of the lithium-like ions k with continuum electrons. Thus this process provides an indirect or virtual contribution to deexcitation, the DL deexcitation, to be added to the ordinary direct deexcitation. The DL deexcitation rate coefficient $F_{\mathrm{DL}}(k \rightarrow i)$ is related to $C_{\mathrm{DL}}(i \rightarrow k)$ by the principle of detailed balance [2]

$$F_{\mathrm{DL}}(k \rightarrow i) = g(i)/g(k)\, C_{\mathrm{DL}}(i \rightarrow k) \exp[E(i,k)/kT_e]. \tag{4}$$

It is noted that Eq. (4) is exactly the same as the relation holding for the rate coefficients for the ordinary direct excitation and deexcitation processes.

We include the DL excitation and deexcitation for the $n=2$–3, 2–4, 2–5, and 3–5 transitions and the $2s\ ^2S-2p\ ^2P$ transition of lithiumlike aluminum ions, where n is the principal quantum number. The excitation cross-section data have been calculated by Zhang, Sampson, and Fontes [13] for the transitions from the ground state ($2s\ ^2S$) and the $2p\ ^2P$ level, and for other transitions; the cross sections have been calculated in the distorted-wave approximation, the details of which are given in Ref. [14].

In Fig. 2, the thick solid and dotted lines show the n_e dependences of the DL deexcitation rate coefficients for the $2s\ ^2S-3p\ ^2P$ and $2s\ ^2S-3d\ ^2D$ transitions, respectively, which are calculated from Eqs. (3) and (4). The direct collisional deexcitation rate coefficients of these transitions are given by the horizontal lines. As the electron density increases, the generalized Griem boundary level is lowered and the DL deexcitation rate coefficient increases. For $n_e>10^{25}$ m^{-3}, the rate coefficients of the DL process become larger than those of the direct process. For $n_e>10^{27}$ m^{-3}, the DL deexcitation rate coefficients become constant; this is because, in this region, p_C is given by p_B and is independent of n_e.

III. CORE ELECTRON TRANSITION AND CAPTURED ELECTRON TRANSITION (CR RECOMBINATION FROM EXCITED IONS)

In addition to the DL processes, we consider another process involving doubly excited levels: The radiative or collisional deexcitation of the core electron $(k,p)\rightarrow(i,p)+h\nu$ or $(k,p)+e\rightarrow(i,p)+e$ $(i<k)$ from a level with $p>p_C$ may enhance the transition $k\rightarrow i$ because these doubly excited levels are strongly coupled with the parent and continuum states. (See the thick dotted arrow in Fig. 1.) If we approximate the radiative decay probability $A_{\mathrm{core}}(k\rightarrow i)$ and collisional deexcitation rate coefficient $F_{\mathrm{core}}(k\rightarrow i)$ of the transition $(k,p)\rightarrow(i,p)$ using the corresponding rate constants for the lithiumlike ions, $A(k\rightarrow i)$ and $F(k\rightarrow i)$, respectively, we may express the effective rate as

$$A_{\mathrm{core}}(k\rightarrow i)=\int_{p_C}^{p_{\mathrm{limit}}} n(k,p)_{\mathrm{LTE}}\,dp\ A(k\rightarrow i), \qquad (5)$$

and a similar relationship holds for $F_{\mathrm{core}}(k\rightarrow i)$. Here $n(k,p)_{\mathrm{LTE}}$ denotes the LTE population with unit population density in level k and p_{limit} is determined by ''the ionization potential lowering.'' For hydrogen atoms, Shimamura and Fujimoto [15] introduced an ion sphere model with the radius $r_i=(3/4\pi n_e)^{1/3}$ and derived that the upper limit and the number of the bound levels were given by $n^*=(2.0\times10^{29}\ \mathrm{m}^{-3}/n_e)^{1/6}$ and $N_{\mathrm{bound}}=(1.7\times10^{29}\ \mathrm{m}^{-3}/n_e)^{1/2}$, respectively. We scale the radius r_i by n_e/z_{eff}, i.e., p_{limit} is expressed as $(2.0\times10^{29}\ z_{\mathrm{eff}}^4\ \mathrm{m}^{-3}/n_e)^{1/6}$, where z_{eff} $(=10)$ is the effective nuclear charge of the berylliumlike aluminum ions. The integral in Eq. (5) takes into account the LTE populations of the doubly excited levels associated with the level k of lithiumlike ions. Since the number of doubly excited levels and the population of each level in LTE are proportional to $n_e^{-1/2}$ and n_e, respectively, the integral in Eq. (5) is proportional to $n_e^{1/2}$. In the electron density region of $n_e<10^{27}$ m^{-3}, the fraction of the LTE populations with respect to the population of the parent level k is less than 10% for $T_e=30$ eV. It may be concluded that the contribution from the core electron transition is rather insignificant.

In the above, we have expressed the core electron transition as an enhancement of the transition $k\rightarrow i$. However, since the LTE populations associated with the parent level k are strongly coupled with this level, the core electron transition may be interpreted as an effective enhancement of the population $n(k)$ of the parent level k. The degree of enhancement depends on the parent level.

A third process to be considered is a multistep transition involving the captured electron, a process similar to the standard collisional-radiative (CR) recombination process, established for the ground-state ions [12,16]. Its essential feature in the present context is that the populations of the high-lying levels (k,p), which are in LTE with respect to the level k, are lost by deexcitation of the captured electron p. The mechanism of the CR recombination is summarized as follows. In the low-density region of $p_G>p_B$ [in this description, we use p in place of (k,p)], the CR recombination rate is the sum of the direct radiative recombination rate to levels $q<p_G$ and the radiative cascade rate from the levels $p>p_G$ to these low-lying levels q. In the high-density region of $p_G<p_B$ the rate is determined by the mutlistep ladderlike deexcitation flow originating from the start of the ladder p_B; the CR recombination rate is approximately given by $n(p_B)F(p_B,p_B-1)n_e$, where $n(p_B)$ may be approximated by the LTE population. (See Figs. 5–7 and 10 in Ref. [12].) In the following we approximate the CR recombination rate coefficient for excited lithiumlike ions by that for the ground-state heliumlike ion with effective core charge $z_{\mathrm{eff}}=10$ (nuclear charge 12). In the first example treated in Sec. IV, the density region corresponds to the case of $p_G>p_B$ (see Fig. 2) and the CR recombination rate coefficient will depend on the details of the ionic states and the energy-level structure of the doubly excited ions. Therefore, our approximation may slightly over- or underestimate the actual rate coefficient. On the other hand, in the second example, since $p_G<p_B$ $(=9.5)$, the rate coefficient will be insensitive to the details of the energy-level structure in the energy range lower than p_B. In this case, our estimate should be fairly accurate.

In Fig. 2, the thick dash-dotted line represents the rate coefficient of the CR recombination from the ground-state heliumlike ions with $z_{\mathrm{eff}}=10$. We include in our CR model code the core electron transitions among the $n\leqslant5$ levels and the CR recombination from levels with $n\leqslant8$.

IV. CALCULATION OF THE EXCITED LEVEL POPULATIONS AND THE GAINS FOR A LITHIUMLIKE ALUMINUM ION LASER

We took into account these three additional processes into our CR model code [7] for lithiumlike ions and we calculated the populations and gains for a lithiumlike aluminum ion x-ray laser scheme. We assume $T_e=30$ eV, which is a typical temperature derived from hydrodynamics simulation for the laser-produced aluminum plasma [3,4,17], and that the plasma is in the recombining plasma scheme, i.e., the excited level populations are created only from heliumlike ions. The heliumlike ground-state ion density was assumed

to be 10% of the electron density. The line profile of the laser transitions was assumed to be a Gaussian and the ion temperature was assumed to be equal to the electron temperature. For the doubly excited levels whose captured electron has the same principal quantum number as that of a core electron, e.g., $1s^2nlnl'$ levels, a precaution was taken not to double count the atomic processes via these levels. The atomic processes originating from the excited heliumlike ions were ignored because, in the present example, the maximum electron temperature during the production of the plasma is ~300 eV and populations in the excited levels of heliumlike ions are expected to be rather small. (The excitation threshold of $1s^2\ ^1S-1s2p\ ^1P$ of helium like aluminum ions is about 1300 eV.)

Figure 3 shows examples of the populations of several excited levels calculated (a) without and (b) with the additional processes taken into account. These populations per unit statistical weight have been further divided by the heliumlike ground-state ion density and the electron density. In the region of $n_e=10^{24}-10^{26}$ m^{-3}, i.e., the gain region for the aluminum laser, we find no drastic change in the populations, although in this region the rates of the DL deexcitation and the recombination are comparable to or even larger than those of the direct process, as seen from Fig. 2. In this density region, the $n=5$ levels are almost in LTE and the dominant population and depopulation processes into or out of the $n=4$ levels are collisional l changing, collisional transition from and into the $n=5$ levels, and the radiative process. The $n=3$ levels are populated mainly by radiative cascade from higher-lying levels and depopulated by radiative decay into the lower levels [7]. For all the cases, the collisional DL deexcitations and the recombination play only minor roles.

As seen from Fig. 3(b), in the electron density region of $10^{26}-10^{27}$ m^{-3}, the excited level populations decrease in comparison to those shown in Fig. 3(a). In this density region, the rate coefficient of the DL processes is saturated, leaving as the dominant process the recombination from excited levels. (See Fig. 2.) This is because the recombination rate coefficient is almost proportional to n_e in this high-density region. Since we assume the plasma to be purely recombining, the rapid depopulation by recombination is not compensated by the downward population flow through the singly excited levels. In the absence of the additional processes, since Byron's boundary level is 4.2, the $n=3$ and 4 levels are in the ladderlike deexcitation flow [18]. Thus the effect of the additional process is strong for these levels. However, the $n=5$ levels are in near LTE, or strongly coupled with the heliumlike ground-state ion, which would result in a slight deviation from an LTE population.

Figure 4 shows the amplification gains of several transitions corresponding to the assumptions used in Fig. 3. As one can see, no significant change has been brought about by the introduction of the additional processes.

Several years ago, Moreno *et al.* [19] measured the linewidth and the amplification gain of the $3d\ ^2D_{5/2}-5f\ ^2F_{7/2}$ line of lithiumlike aluminum ions and derived a population inversion of $(1.2\pm0.3)\times10^{23}$ m^{-3} and an electron density of 3.3×10^{25} m^{-3}. This, together with the assumptions that the heliumlike ground-state ion density is about 3×10^{24} m^{-3} ($\sim0.1n_e$) and the $5f\ ^2F_{7/2}$ level is almost in LTE with respect to the heliumlike ground-state ions and continuum

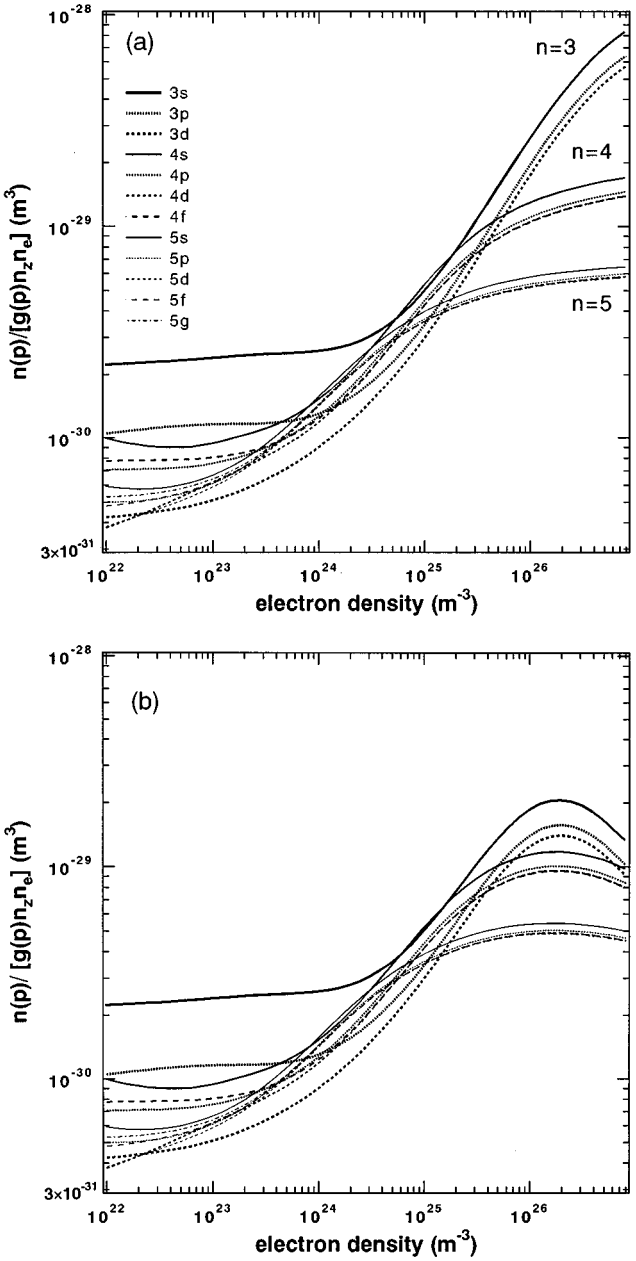

FIG. 3. Excited level populations of several excited levels of lithiumlike aluminum ions in the recombining plasma: (a) additional processes are not included and (b) additional processes are included.

states, leads to an estimate of the electron temperature around 5 eV. Thus it is worth considering the lower-temperature case. We took therefore $T_e=5$ eV and performed a calculation similar to that of the case of $T_e=30$ eV. Figure 5 shows the rate coefficients of the DL deexcitation and the recombination from the excited levels. The increases in the rate coefficients of the DL deexcitation and the recombination in comparison with Fig. 2 stem from the increase in the LTE populations associated with the parent level at this low electron temperature. Figure 6, corresponding to Fig. 3(b), shows the excited level populations of the $n=3$, 4, and 5 levels calculated with the additional processes included. For $n_e\geqslant3\times10^{24}$ m^{-3}, the populations of the $n=3$, 4, and even 5 levels decrease rapidly, a consequence of the en-

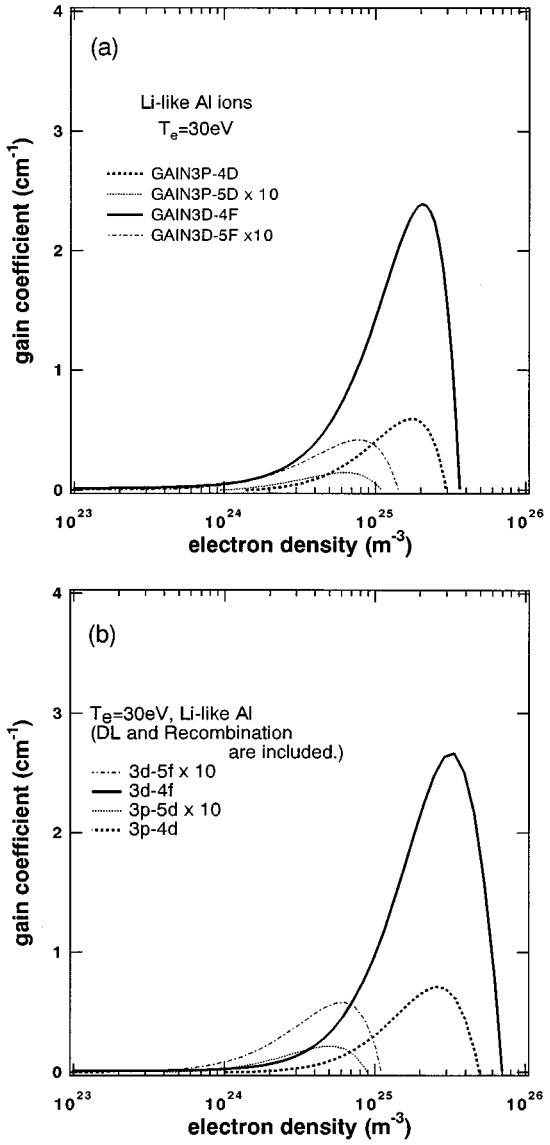

FIG. 4. Amplification gains of several lasing transitions of lithiumlike aluminum ions: (a) additional atomic processes are not included and (b) additional processes are included. The gains for the $n=3-5$ transitions have been multiplied by 10.

hancement of the recombination by at least one order of magnitude over the DL deexcitation rate in this electron density region. (See Figs. 5 and 8.) It should be noted that the population inversions on the $3d\ ^2D_{5/2}-5f\ ^2F_{7/2}$ and $3d\ ^2D_{5/2}-4f\ ^2F_{7/2}$ lines at $n_e=3\times10^{25}$ m^{-3} are 4.7×10^{22} and 1.5×10^{21} m^{-3}, respectively, consistent within a factor of 3 with the experimental result in Ref. [19]: The calculated result is 2.5 times smaller than the experimental value for the $3d\ ^2D_{5/2}-5f\ ^2F_{7/2}$ line and 1.4 times larger for the $3d\ ^2D_{5/2}-4f\ ^2F_{7/2}$ line.

We calculated the amplification gain under these conditions; at this temperature, the line profile of the laser transitions is determined by the Stark rather than Doppler broadening. For the case of the $3d\ ^2D_{5/2}-4f\ ^2F_{7/2}$ transition at $n_e=10^{25}$ m^{-3}, the Doppler and Stark widths derived from the impact approximation are 2×10^{12} and 9×10^{12} s^{-1}, respectively [20]. For the 3–5 transitions, we have to apply the linear Stark broadening [19], e.g., the Stark width of the

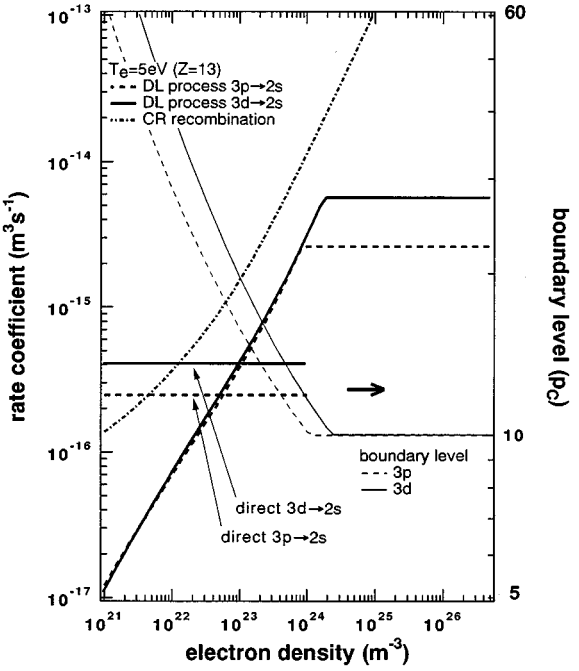

FIG. 5. DL deexcitation and the recombination rate coefficient from an excited level for $T_e=5$ eV. Other explanations are the same as in Fig. 2.

$3d\ ^2D_{5/2}-5f\ ^2F_{7/2}$ is 6×10^{13} s^{-1} at $n_e=10^{25}$ m^{-3}. Thus we assume the Doppler broadening for $n_e<2\times10^{24}$ m^{-3} and the Stark broadening for $n_e\geqslant2\times10^{24}$ m^{-3}. The result of the calculated gains is shown in Fig. 7. At $n_e=3\times10^{25}$ m^{-3}, the gains of the $3d\ ^2D_{5/2}-5f\ ^2F_{7/2}$ and $3d\ ^2D_{5/2}-4f\ ^2F_{7/2}$ lines are 1.8 and 6.3 cm^{-1}, respectively. The former is consistent with the experiments [3–5,19] in which the gain coefficients were $g=1.63-3.5$ cm^{-1}. For

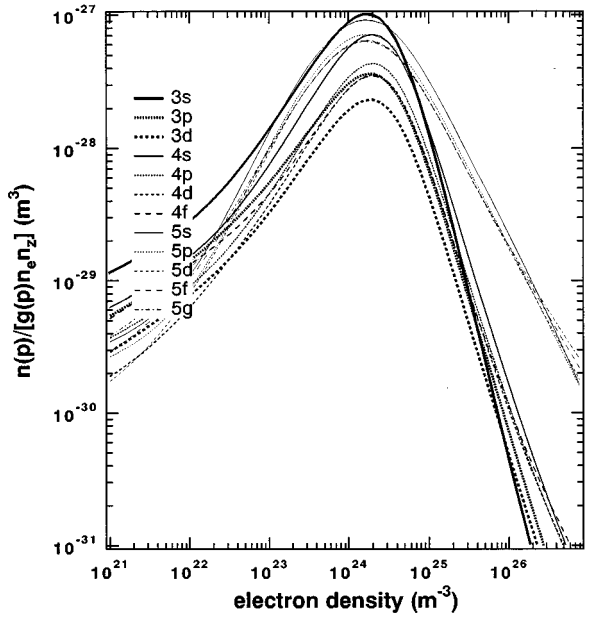

FIG. 6. Excited level populations of several excited levels of lithiumlike aluminum ions in the recombining plasma with $T_e=5$ eV. Additional processes are included.

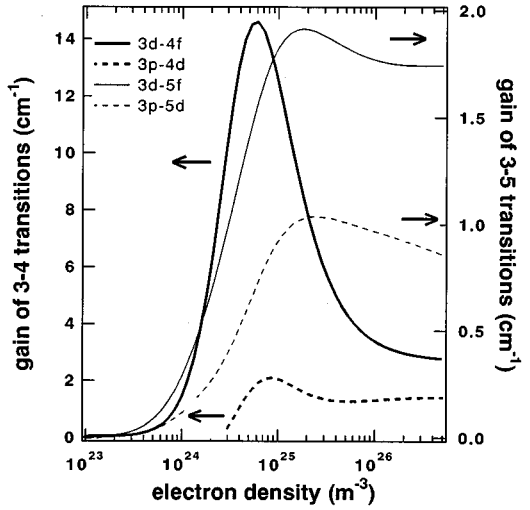

FIG. 7. Calculated gains of several transitions of lithiumlike aluminum ions with the additional processes included. The gains for the $n=3-4$ transitions are labeled on the left-hand side ordinate and those for the $n=3-5$ transitions are on the right-hand side ordinate.

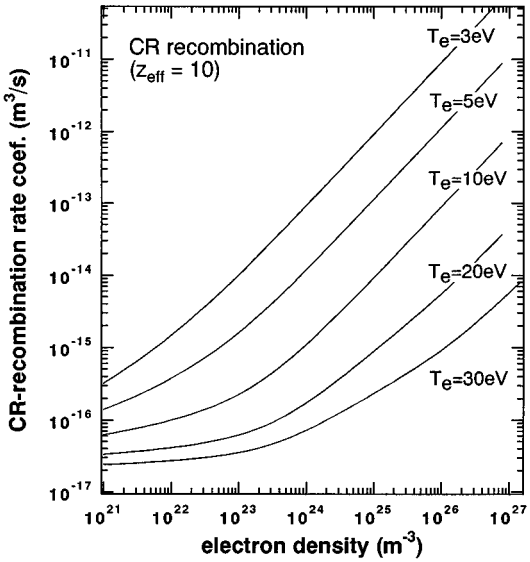

FIG. 8. Calculated CR recombination rate coefficients from the ground-state heliumlike ions with $z_{\rm eff}=10$ for various electron temperatures.

the $3d\ ^2D_{5/2}-4f\ ^2F_{7/2}$ line, our result is about 1.3–2.3 times larger than the experimental gains of 2.56–4.5 cm^{-1}.

V. CONCLUSION

In conclusion, in the present study we have examined the effect of the three additional processes involving doubly excited levels on the population kinetics of the singly excited levels, by adopting rather simple approximations. There appears to be no positive reason why the population kinetics of the *doubly* excited levels would not be affected by the processes involving *triply* excited levels, which we did not include. In view of these facts, our present conclusion should be regarded as rather preliminary. We cannot conclude whether the large gains predicted for the $3d\ ^2D_{5/2}-4f\ ^2F_{7/2}$ transition around $n_e\sim10^{25}$ m^{-3} (Fig. 7) are real or simply a result of our inadequate approximations. However, it is worth noting the following fact: As shown in Fig. 6, in the region where $n_e>5\times10^{24}$ m^{-3}, the $n=5$ populations are larger by one order of magnitude than those of $n=3$ and 4, whereas the $n=4$ populations are only slightly larger than those of $n=3$. This means that small computational errors or a radiation trapping effect on the $2p\ ^2P-3d\ ^2D$ line affect the population inversion density of the $3d\ ^2D_{5/2}-4f\ ^2F_{7/2}$ transition much more than that of the $3d\ ^2D_{5/2}-5f\ ^2F_{7/2}$ transition. For example, at $n_e=3\times10^{25}$ m^{-3}, if the $3d\ ^2D$ population increases by 20%, the population inversion density of the $3d\ ^2D_{5/2}-5f\ ^2F_{7/2}$ transition decreases by only 2%, whereas that of the $3d\ ^2D_{5/2}-4f\ ^2F_{7/2}$ transition decreases by 50%.

ACKNOWLEDGMENT

This work was partially supported by RIKEN (special postdoctoral researchers program).

APPENDIX: CR RECOMBINATION FROM EXCITED LEVELS

Figure 8 shows the CR recombination rate coefficients from the ground-state heliumlike ions with $z_{\rm eff}=10$. (See Sec. III.) In this calculation, for the electron impact excitation and deexcitation rate coefficients among the $n\geqslant6$ levels, we use the semiempirical formulas for hydrogenic ions by Sampson and Zhang [21]. The other atomic data that we used in our model are described in Ref. [7].

[1] T. Fujimoto and T. Kato, Phys. Rev. Lett. **48**, 1022 (1982).
[2] T. Fujimoto and T. Kato, Phys. Rev. A **32**, 1663 (1985).
[3] P. Jaeglé, G. Jamelot, A. Carillon, A. Klisnick, A. Sureau, and H. Guennou, J. Opt. Soc. Am. B **4**, 563 (1987).
[4] A. Calliron, M. J. Edwards, M. Grande, M. J. de C. Henshaw, P. Jaeglé, G. Jamelot, M. H. Key, G. P. Kiehn, A. Klisnick, C. L. S. Lewis, D. O'Neill, G. J. Pert, S. A Ramsden, C. M. E. Regan, S. J. Rose, R. Smith, and O. Willi, J. Phys. B **23**, 147 (1990).
[5] T. Hara, K. Ando, N. Kusakabe, H. Yashiro, and Y. Aoyagi, Jpn. J. Appl. Phys. **28**, L1010 (1989).
[6] A. Klisnick, A. Sureau, H. Guennou, H. C. Moller, and J. Virmont, Appl. Phys. B **50**, 153 (1990).
[7] T. Kawachi, T. Fujimoto, and G. Csanak, Phys. Rev. E **51**, 1428 (1995); T. Kawachi and T. Fujimoto, *ibid.* **51**, 1440 (1995).
[8] V. L. Jacobs and J. Davis, Phys. Rev. A **18**, 697 (1978).
[9] T. Fujimoto, J. Phys. Soc. Jpn. **47**, 273 (1979).

[10] H. R. Griem, *Plasma Spectroscopy* (McGraw-Hill, New York, 1964), p. 129.
[11] S. Byron, R. C. Stabler, and P. I. Bortz, Phys. Rev. Lett. **8**, 376 (1967).
[12] T. Fujimoto, J. Phys. Soc. Jpn. **49**, 1569 (1980).
[13] H. L. Zhang, D. H. Sampson, and C. J. Fontes, At. Data Nucl. Data Tables **44**, 31 (1989).
[14] R. E. H. Clark, G. Csanak, and J. Abdallah, Jr., Phys. Rev. A **44**, 2874 (1991).
[15] I. Shimamura and T. Fujimoto, Phys. Rev. A **42**, 2346 (1990).
[16] T. Fujimoto, J. Phys. Soc. Jpn. **49**, 1561 (1980).
[17] In Ref. [3], the $T_e = 48$ eV is adopted as a typical temperature; in Ref. [4], the gains are calculated under the condition $T_e = 20$ eV.
[18] T. Fujimoto, J. Phys. Soc. Jpn. **47**, 265 (1979).
[19] J. C. Moreno, H. R. Griem, S. Goldsmith, and J. Knauer, Phys. Rev. A **39**, 6033 (1989).
[20] I. I. Sobelmann, L. A. Vainshtein, and E. A. Yukov, *Excitation of Atoms and Broadening of Spectral Lines* (Springer-Verlag, Berlin, 1981).
[21] D. H. Sampson and H. L. Zhang, Astrophys. J. **335**, 516 (1988).